Instabilities in Josephson ladders with current induced magnetic fields

B. R. Trees and R. A. Murgescu
Department of Physics and Astronomy, Ohio Wesleyan University, Delaware, Ohio 43015
(Received 6 October 2000; revised manuscript received 28 December 2000; published 16 March 2001)

We report on a theoretical analysis, consisting of both numerical and analytic work, of the stability of synchronization of a ladder array of Josephson junctions under the influence of current induced magnetic fields. Surprisingly, we find that as the ratio of the mutual to self-inductance of the cells of the array is increased a region of unstable behavior occurs followed by reentrant stable synchronization. Analytic work tells us that in order to understand fully the cause of the observed instabilities the behavior of the vertical junctions, sometimes ignored in analytic analyses of ladder arrays, must be taken into account.

DOI: 10.1103/PhysRevB.63.144503 PACS number(s): 74.50.+r, 05.45.Xt, 05.45.−a

Ladder arrays of Josephson junctions are intriguing systems for a wealth of reasons: the possibility of phase locking, or synchronizing, a maximal subset of junctions suggests their use as microwave sources;[1] they offer rich dynamical behavior, accessible to both theorists and experimentalists, in the field of coupled nonlinear oscillators (with recent interest in the prediction and observation of discrete rotobreathers);[2] their complexity is between that of better understood one dimensional serial and parallel arrays and full two-dimensional arrays (e.g., square arrays), and thus they offer a nice link between the two geometries; and ladder arrays can, under circumstances that are partially understood, be modeled by the discrete sine-Gordon (DSG) equation,[3] which is itself a source of research interest among many.[4] With a desire to understand better the conditions under which stable synchronization can occur, we consider ladder arrays with periodic boundary conditions biased with uniform dc bias currents I_B greater than the critical currents of the junctions, and we include the effects of current induced magnetic fields (CIMF's) via self and mutual inductances of the cells of the array (see Fig. 1). Since the array is current-biased above the critical current there will be a nonzero voltage across some subset of junctions in the array. These ''active'' junctions are synchronized, or phase locked, if their voltages, after some initial transients, are identical functions of time. Furthermore, previous workers have established that the effects of CIMF's may be important[5] in determining the static and dynamics properties of arrays, and so it is natural to consider the effects of CIMF's on synchronization as well.

In this paper we present numerical and analytical evidence that mutual inductance between cells of a ladder array can lead to rich dynamical behavior, including destabilization of synchronization and reentrant synchronization as the relative size of the mutual to self inductance of the cells is increased. The instability results for a finite range of values of the mutual inductance and occurs when, for the resistively and capacitively shunted junction (RCSJ) model, the numerical solutions to the model equations diverge with time. In addition to our numerical solutions we also investigate the dynamics analytically. Namely, the two coupled RCSJ equations for the horizontal and vertical junctions can be approximately decoupled. The simplified equations allow us to calculate analytically the Floquet exponents, which measure the degree of stability of the synchronization. Then, by direct comparison of the analytic results for the Floquet exponents, based on the simplified equations, and the numerical results for the Floquet exponents, based on the full RCSJ equations, we learn valuable information about the roles of the horizontal and vertical junctions in the array. This technique appears to be a powerful way to analyze the relative importance of subsets of junctions that experience different local conditions.

Josephson junctions consist of superconducting islands separated by a thin layer of nonsuperconducting material. In the superconductors, the coherent motion of the paired electrons, or Cooper pairs, leads to a wavefunction of the form $\Psi=|\Psi|e^{i\theta}$, where θ is the macroscopic phase of the superconductor. The equations describing the dynamics of a single junction depend on the gauge-invariant phase *difference*, or Josephson phase, across the junction, $\phi=\theta_1-\theta_2-(2\pi/\Phi_0)\int_1^2\mathbf{A}\cdot d\mathbf{l}$, where $\mathbf{A}$, the vector potential due to an external magnetic field, is integrated along a path from one side of the junction to the other. $\Phi_0=\hbar/2e$ is the magnetic flux quantum, where $\hbar$ is Planck's constant divided by 2π and e is the electronic charge. We assume in this work that $\mathbf{A}=0$.

Consider a ladder array of underdamped junctions with N cells and periodic boundary conditions, as shown in Fig. 1. Each junction has a McCumber parameter $\beta_c\equiv 2\pi CI_{cx}R^2/\Phi_0$, where $C(R)$ is the junction's capacitance (resistance), and I_{cx} is the critical current of a ''horizontal'' junction. We assume each cell of four junctions is described by a self-inductance L and also has a mutual inductance $-M$ $(M>0)$ with each of its two nearest neighbors, where $M<L$. As an adjustable parameter in the theory, M/L is allowed to range between zero and one. Basic physics arguments for a simple ladder with nearest-neighbor mutual inductance precludes M/L from exceeding 0.5.[6] Nevertheless, it is informative and worthwhile to study the behavior of the model equations over the range $0<M/L<1$. Furthermore, such theoretical work could pique the interest of others to try, using modern fabrication techniques, to enhance the mutual over the self-inductance of the cells and thereby probe the broader range of M/L values studied here. Alternatively, one could point to these results for $M/L>0.5$ as an interesting portent to the behavior that might be observed in arrays with overlapping cells or in three-dimensional arrays.

An analysis based on the RCSJ equations and including

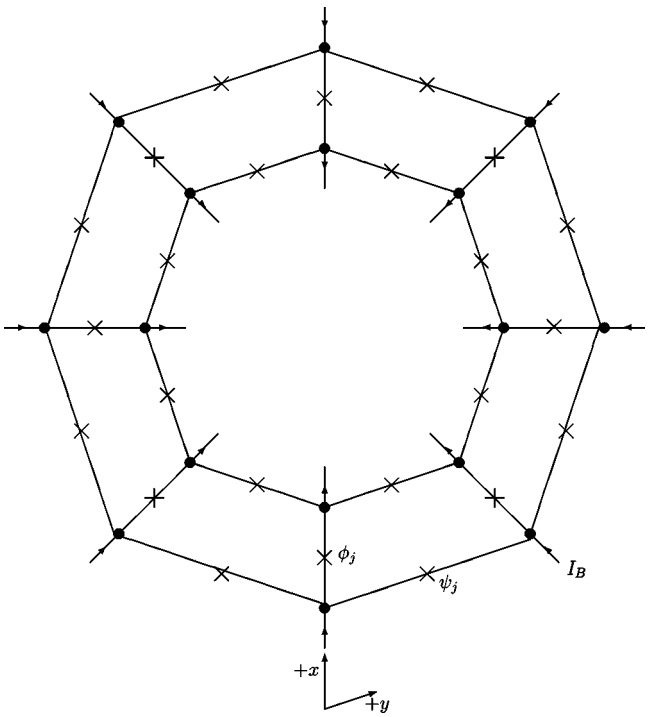

FIG. 1. Ladder array of Josephson junctions with periodic boundary conditions. The horizontal junctions, along the rungs of the ladder, are parallel to the *x* axis, while the vertical junctions are parallel to the *y* axis. A dc bias current, I_B, is injected at each node on one side and extracted from the opposite side. The Josephson phase for the horizontal (vertical) junction in the *j*th plaquette is ϕ_j (ψ_j).

the effect of induced magnetic flux leads to a pair of coupled equations for the Josephson phases of the horizontal and vertical junctions,

$$\beta_c \phi'' + \phi' + \sin\phi + \frac{1}{\beta_L} \underline{Z}^{\mathrm{Tr}} \cdot \underline{X}^{-1} \cdot (\underline{Z} \cdot \phi + 2\psi) = 0, \quad (1)$$

$$\beta_c \psi'' + \psi' + \alpha \sin\psi + \frac{1}{\beta_L} \underline{X}^{-1} \cdot (\underline{Z} \cdot \phi + 2\psi) = 0, \quad (2)$$

where $\beta_L \equiv 2\pi L I_{cx}/\Phi_0$ is the dimensionless self-inductance of a cell, and $\alpha \equiv I_{cy}/I_{cx}$ is the critical current anisotropy. All our work presented here corresponds to $\alpha = 1$. The prime symbols denote differentiation with respect to dimensionless time, $\tau \equiv t/t_c$ where $t_c \equiv \hbar/2eI_{cx}R$. These equations are compactly represented in matrix notation, where ϕ and ψ are *N*-dimensional vectors representing the Josephson phases of the horizontal and vertical junctions, respectively. $\underline{Z}$ is an $N \times N$ matrix that depends on geometry, and $\underline{X}$ is the dimensionless inductance matrix, also $N \times N$ in size. The diagonal terms of $\underline{X}$ represent the self-inductance of a given cell, i.e., $X_{jj} = +1$, while the mutual inductance of the nearest-neighbor cells is represented by the terms $X_{j,j\pm1} = -\mu_L$, where $\mu_L \equiv M/L$ is the dimensionless mutual inductance. All other elements of $\underline{X}$ are zero. Equations (1) and (2) were solved numerically for ϕ, ψ, ϕ', and ψ' via a fourth-order Runge-Kutta algorithm as a function of the parameters *N*, β_c, β_L, μ_L, and $i_B \equiv I_B/I_{cx}$ (the dimensionless bias current). The starting configuration consisted of random voltages and zero Josephson phases.

As described elsewhere for a similar system[7] a stability analysis of the solutions to Eqs. (1) and (2) follows by letting $\phi = \phi_0 + \eta$ and $\psi = \psi_0 + \delta$, where ϕ_0 and ψ_0 are solutions to these equations. Equations (1) and (2) are linearized with respect to η and δ. The time dependence of the perturbations has the form $\eta \sim e^{\lambda t_c \tau}$ and $\delta \sim e^{\Lambda t_c \tau}$, where λ (Λ) represent the Floquet exponents for the horizontal (vertical) junctions. If $\mathrm{Re}(\lambda t_c) > 0$ or $\mathrm{Re}(\Lambda t_c) > 0$ we expect unstable behavior of the array for the given set of circuit parameters. In fact, we are interested in that exponent whose magnitude is closest to zero, as that describes the stability of the longest-lived mode of the array.

Figure 2(a) shows the minimum Floquet exponent as a function of μ_L for a 5-cell ladder. The symbols are results of a numerical stability analysis of Eqs. 1 and 2. The meaning of the error bars visible in the figure requires some explanation. For the values of dimensionless capacitance ($\beta_c = 10$) and dimensionless self-inductance ($\beta_L = 100$) used here, the array exhibits interesting behavior when its phase-locked solutions are perturbed. In fact, the numerically calculated Floquet exponents are a relatively weak function of the run time of the code. That is, as the number of time steps employed in the Runge-Kutta method is systematically increased, the numerically calculated exponents oscillate about a well-defined mean value. The size of the oscillations is small, with a standard deviation of the mean, for a sample of eight to ten different run times, that is about one percent of the mean value of the exponent. Such behavior of Josephson junction arrays has been previously observed[7] and is characteristic of arrays that are only weakly stable. (Note the small magnitude of λ_{min}.) In addition to the weak dependence of the exponents on the run time of the code, we also found a weak dependence of the exponents on the initial values of the voltages, ϕ' and ψ'. We therefore *also* averaged the numerically calculated exponents over eight to ten different sets of randomly assigned initial voltages. The results in Figs. 2(a), 2(b), and 2(c) then represent a double average, for each value of μ_L, over run time and initial voltage. The error bars represent the standard deviation of the mean of the resulting set of exponents for each value of μ_L. The small size of the error bars, which are clearly less than the size of the symbols themselves, implies that these averaged results are indeed meaningful.

Based on Fig. 2(a), we see that as μ_L is increased from zero towards 0.5, the stability of phase locking increases, as shown by the negative exponent of growing magnitude, while the degree of stability decreases for increasing μ_L greater than approximately 0.6. Even more interesting is the behavior of the ladder in the range $0.5 \lesssim \mu_L \lesssim 0.6$. For these values of the mutual inductance the ladder is actually unstable. This is evidenced by very rapidly growing phases and voltages with time as Eqs. (1) and (2) are numerically integrated. For $N = 5$, the lower limit of this instability region is $\mu_L^{(1)} = 0.5$ independent of other circuit parameters such as β_c and β_L. The upper limit of this region, which we denote by

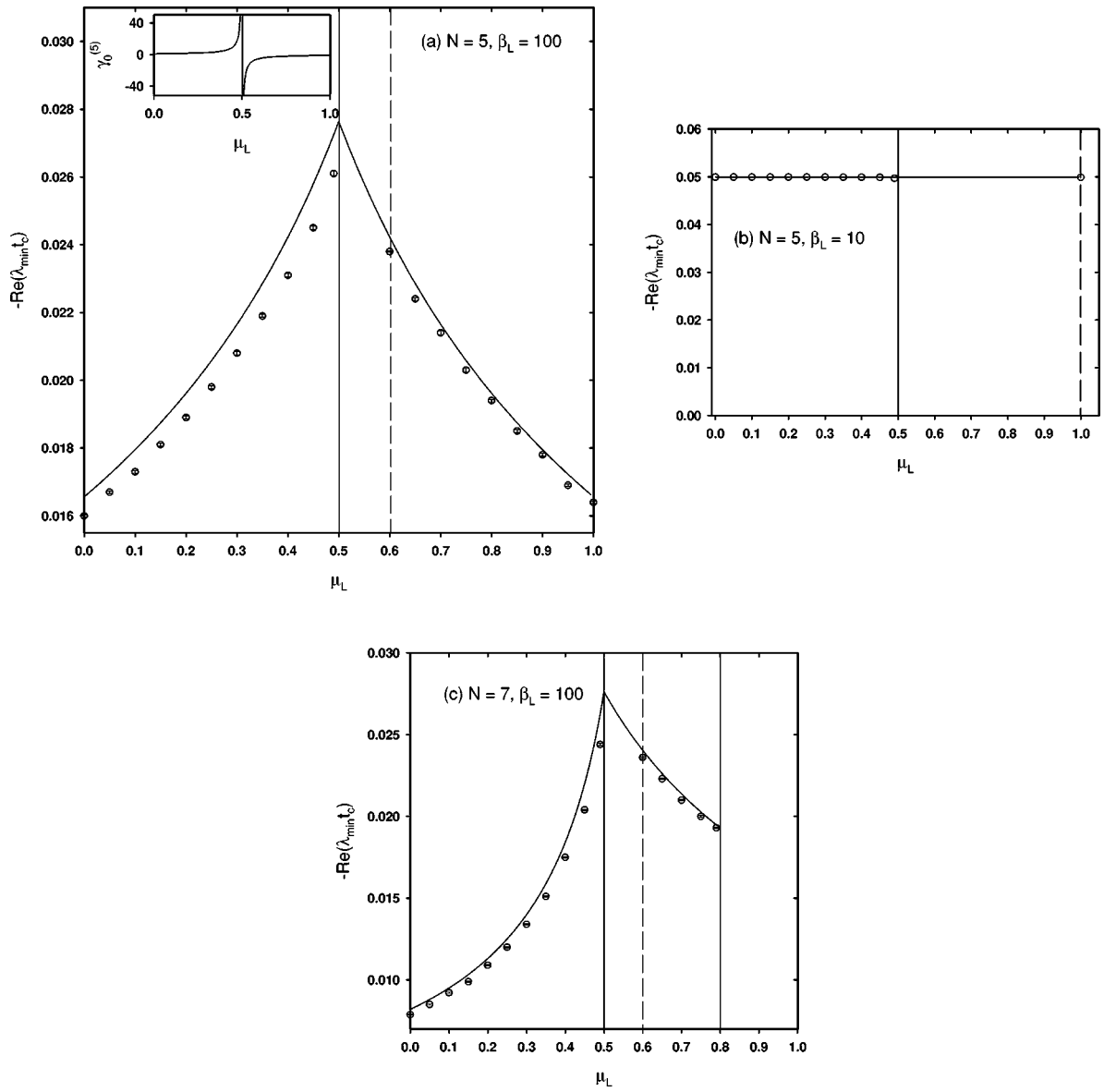

FIG. 2. Minimum Floquet exponent for periodic ladders versus the dimensionless, nearest-neighbor mutual inductance. The circular symbols with error bars are the results of a numerical stability analysis based on Eqs. (1) and (2). Each circle is an average over different values of the run time of the code and also different values of the initial voltages. The error bars represent the standard deviation of the mean exponent. Each circle represents an average of a set of eight to ten different (random) initial voltages, where for each particular set of initial voltages, the Floquet exponents for fifteen different run times were calculated. The solid line represents an analytic result [Eq. (3)] based on the horizontal junctions. (a) $N=5$, $i_B=10$, $\beta_c=10$, and $\beta_L=100$. The analytic result predicts stable phase-locked solutions for $0\leqslant\mu_L\leqslant 1$. The numerical results exhibit an instability, however, for $\mu_L^{(1)}\leqslant\mu_L\leqslant\mu_L^{(2)}$, where $\mu_L^{(1)}=0.5$ and $\mu_L^{(2)}$ is dependent on the starting configuration of phases and voltages, as well as on the value of β_L. The region is denoted by vertical lines on the graph. The dotted vertical line represents that the upper boundary of the instability region is not well defined for these average exponents. This instability originates with the vertical junctions. INSET: geometric quantity $\gamma_0^{(5)}$ versus μ_L. [See Eq. (4).] (b) $N=5$, $i_B=10$, $\beta_c=10$, and $\beta_L=10$. Decreasing the self-inductance has resulted in more stable phase locking for $\mu_L<0.5$, in which region, additionally, the exponents equal $-1/2\beta_c$, independent of μ_L. But the instability region for $\mu_L>0.5$ has grown significantly due to the decrease in the value of β_L. (c) $N=7$, $i_B=10$, $\beta_c=10$, and $\beta_L=100$. In this case, the geometry of the ladder leads to an instability for $\mu_L>0.8$ that originates with the horizontal junctions. The boundary of this ''large μ_L'' instability is marked in the figure with a vertical line at $\mu_L=0.8$. The instability due to the *vertical* junctions near $\mu_L=0.5$ still exists, as it did in the ladder with $N=5$.

$\mu_L^{(2)}$, depends on such quantities as the value of the starting voltages as well as on the value of β_L. For example, for a fixed set of starting voltages, we find that $\mu_L^{(2)}$ is a decreasing function of β_L. We have denoted the variability of the value of $\mu_L^{(2)}$ by drawing a dotted vertical line in the figure. Such a line is meant to convey merely that the upper boundary of the instability region is not well defined for these averaged exponents. In any event, precise knowledge of $\mu_L^{(2)}$

is not crucial here, but the knowledge that the instability region exists *is* important. Also, it is interesting to note that this instability region does not appear at all if both the phases *and* the voltages are initialized to zero! (See discussion below for the reason for this behavior.)

Physically, this instability is due to a competition between the self-inductance of a given loop (say loop j), which wishes to have a current with a given sense of circulation, and the mutual inductance of the two neighboring loops ($j \pm 1$), which wish to have the current in loop j flow in the opposite sense. We have also looked at ladders with $N=6$, 7, 8, and 9. All show this instability in the vicinity of $\mu_L = 0.5$. Indeed, we would expect this competition-induced instability to be independent of ladder size for the case of nearest-neighbor mutual inductance in that the onset of the instability should always occur at $\mu_L = 0.5$.

If, for $N=5$, we reduce the value of the dimensionless self-inductance such that $\beta_L = 10$ and keep $\beta_c = 10$, then for $\mu_L < 0.5$ the phase-locked solutions are more stable, as shown by the larger value of $|\lambda_{min}|$ seen in Fig. 2(b). Furthermore, the weak dependence of the numerically calculated exponents on run time and initial voltage disappears completely, as evidenced by the lack of error bars in the figure. In Fig. 2(b) we see that for $\mu_L < 0.5$ the exponents equal $-1/2\beta_c$, independent of μ_L, and we also note that the instability region for $\mu_L \gtrsim 0.5$ has increased significantly with the decrease in value of β_L, as mentioned previously.

Interestingly, we find that ladders with $N=7$, 8, and 9 also exhibit a *second* instability region that the 5-cell ladder does not exhibit. Figure 2(c) shows the Floquet exponents for $N=7$. This second instability region has an onset at a value of $\mu_L^{(3)} > \mu_L^{(2)}$ that is dependent on ladder size. We now turn to an analytic calculation of the Floquet exponents, which helps us understand the source of these instabilities.

A reasonable starting approximation is to ignore the coupling between the horizontal and vertical junctions but *otherwise not to ignore the effects of the vertical junctions*. That is, we let $\psi = 0$ in Eq. (1) and $\phi = 0$ in Eq. (2), but we do not then completely ignore Eq. (2) and study only the horizontal junctions. An analysis like that described in Ref. 7 applied to Eq. (1) leads to a Mathieu equation describing the time dependence of the perturbations to the *horizontal* Josephson phases. In such a case, the corresponding Floquet exponents for the horizontal junctions can be calculated analytically. The result is

$$\mathrm{Re}(\lambda_m t_c) = -\frac{1}{2\beta_c} \pm \frac{1}{2\beta_c}\mathrm{Re}\sqrt{1 - 4\omega_m^{(N)}\left(\frac{\beta_c}{\beta_L}\right)}, \qquad (3)$$

where we can think of $\omega_m^{(N)}$ as the *effective* normal-mode frequencies of the ladder with N plaquettes. For example,

$$\omega_m^{(5)} = [4\sin^2(m\pi/N) + 2\mu_L\{\cos(2\pi m/N) - \cos(4\pi m/N)\}]/(\mu_L^2 - \mu_L - 1),$$

where $0 \leq m \leq N-1$. Note that $\omega_m^{(N)}$ is a function of μ_L.

Equation (3) was used to produce the solid curves in Figs. 2(a), 2(b), and 2(c). Note that if, for particular values of $\omega_m^{(N)}$, β_c and β_L, the argument of the square root in Eq. (3) is positive and larger than one, then at least one of the Floquet exponents will be positive, signaling unstable phase-locked solutions. In fact, since $\beta_c > 0$ and $\beta_L > 0$ such an instability will occur if $\omega_m^{(N)} < 0$! Plots of $\omega_1^{(N)}$ versus μ_L for $N=5$ and 7 (not shown here) demonstrate that $\omega_1^{(5)} > 0$ for $0 \leq \mu_L \leq 1$, *but* $\omega_1^{(7)}$ is negative for $\mu_L > 0.8$. We have checked that $\omega_m^{(N)} > 0$ for $m \neq 1$ and for $N=5$ and 7. Thus the cause of this instability in the 7-cell ladder for $\mu_L > \mu_L^{(3)}$ is the $m=1$ normal mode. That is, this instability is a geometrical effect, in that it does not occur for $N=5$, for example, and it is triggered by an effective normal mode frequency of the horizontal junctions becoming negative.

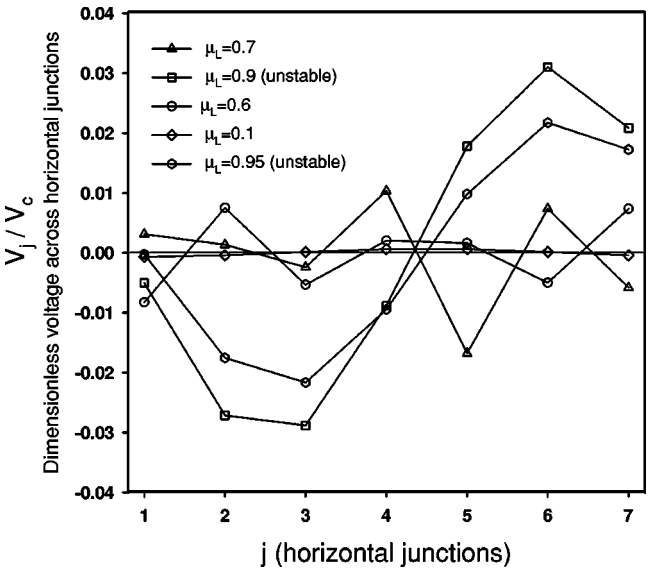

FIG. 3. Characteristic (dimensionless) voltages across the horizontal junctions in a ladder with $N=7$, $i_B=10$, $\beta_c=10$, and $\beta_L=100$. These voltages correspond to the Floquet exponents of smallest magnitude and are plotted as a function of position of the junction along the array. The voltages are actually a subset of the eigenvectors of a matrix used to calculate the Floquet exponents. The characteristic voltages for five different values of the mutual inductance, μ_L, are shown. For the two values of μ_L corresponding to unstable phase locking ($\mu_L = 0.90, 0.95$) there is a noticeable difference in the spatial dependence of the voltages compared to the voltages calculated for $\mu_L = 0.1$, 0.6, and 0.7, for which stable phase locking was observed. The voltages corresponding to the larger values of the mutual inductance tend to have a larger amplitude and to exhibit less spatial variation in sign as one moves along the array. The lines are intended as guides to the eye. (The quantity V_c is defined via $V_c \equiv I_{cx}R$.)

This analytic work, however, does *not* point to the horizontal junctions as the cause of the instability near $\mu_L \gtrsim 0.5$. To appreciate this behavior it is crucial to look to the vertical junctions. A procedure similar to that which led to Eq. (3) leads to a set of effective Floquet exponents for the vertical junctions

$$\mathrm{Re}(\Lambda_m t_c) = -\frac{1}{2\beta_c} \pm \frac{1}{2\beta_c}\sqrt{1 - 4\beta_c\left[\alpha\cos\psi_0 + \frac{2\gamma_m^{(N)}}{\beta_L}\right]}, \quad (4)$$

where the geometrical factor $\gamma_m^{(N)}$ is also a function of μ_L and is similar but not identical to $\omega_m^{(N)}$:

$$\gamma_m^{(5)}(\mu_L)=(\mu_L^4-3\mu_L^2+1)/(1-5\mu_L^2+5\mu_L^4-2\mu_L^5)+\left[2\mu_L(1-\mu_L)\cos\left(\frac{2\pi m}{N}\right)+2\mu_L^2\cos\left(\frac{4\pi m}{N}\right)\right]\Big/(2\mu_L^3-3\mu_L^2-\mu_L+1).$$

In this case, the vertical junctions will exhibit an exponentially growing Josephson phase if $\gamma_m^{(N)}<-(\alpha\beta_L\cos\psi_0)/2$. Now a plot of $\gamma_0^{(5)}$ versus μ_L [see the insert in Fig 2(a)] shows that the function abruptly becomes negative at $\mu_L=0.5$ and asymptotically approaches zero from the negative side as μ_L is increased further. (We have checked that $\gamma_m^{(5)}>0$ for $m\neq 0$. Also, we see similar behavior for the 7-cell ladders.) If we assume that $\cos\psi_0>0$, then the vertical junctions will be unstable for $\gamma_m^{(N)}<0$. Based on the behavior of $\gamma_0^{(5)}$ an instability region will exist for a range of μ_L values, $\mu_L^{(1)}\leqslant\mu_L\leqslant\mu_L^{(2)}$ where $\mu_L^{(1)}=0.5$ and $\mu_L^{(2)}$ will depend on α, β_L, and $\cos\psi_0$. For example, as β_L increases we expect that $\mu_L^{(2)}$ will decrease, i.e., approach a value of 0.5. We have indeed seen such behavior of the numerical results for the Floquet exponents. Also, the inequality $\gamma_m^{(N)}<-(\alpha\beta_L\cos\psi_0)/2$ suggests that the value of $\mu_L^{(2)}$ should depend on the value of $\cos\psi_0$. Recall our discussion of Fig. 2(a), where we noted that the value of $\mu_L^{(2)}$ does indeed depend on the choice of the starting configuration of phases and voltages. In general, then, it is clear that the instability near $\mu_L=0.5$ originates with the *vertical* junctions and would thus be missed by an analysis that was based solely on the horizontal junctions. It is also clear why this instability does not appear numerically when *both* the Josephson phases and the voltages across the junctions are initialized to zero. In such a scenario, although the horizontal junctions may be active, the only possible solution for the vertical junctions is to keep zero voltages and Josephson phases for all times. Since we know this instability region is triggered by the vertical junctions, the vertical junctions have no chance to ''go unstable'' and thus the instability never appears.

We have also studied the characteristic voltages across the horizontal junctions that correspond to particular values of the Floquet exponents. That is, the process of numerically calculating the Floquet exponents involves finding the eigenvalues and eigenvectors of a matrix. The eigenvalues give the values of the Floquet exponents themselves, and thus each particular exponent has a corresponding eigenvector, which in turn represents a set of values for the voltages and Josephson phases for each of the junctions in the array. Thus each eigenvector gives, in a sense, a geometrical picture of the behavior of the junctions for the corresponding Floquet exponent. (see Fig. 3) For a seven-cell ladder we have looked at the eigenvector corresponding to the exponent of minimum size for several different values of μ_L. These numerical results were obtained by initializing all junction voltages and Josephson phases to zero. Figure 3 only shows the voltages across the horizontal junctions because the vertical junctions generally have voltages of two to four orders of magnitude smaller. Careful consideration of the graph, which plots the characteristic voltages as a function of the position of the horizontal junction along the ladder, shows that there is a distinction between the spatial behavior of the voltages for $\mu_L=0.9$ and 0.95 and all the other values of μ_L depicted. For $\mu_L=0.90$ and 0.95, both of which correspond to unstable phase-locking in the seven-cell ladder, the amplitude of the voltages is generally larger and shows less variation of sign as one moves along the array. Those values of the mutual inductance depicted in the graph and for which stable phase locking occur ($\mu_L=0.1,0.6,0.7$) result in voltages of a smaller amplitude which also tend to exhibit greater variations in sign along the ladder. So there does indeed appear to be a geometrical difference in the behavior of the horizontal junctions as μ_L crosses over into the unstable region.

We conclude that mutual inductance between cells of an underdamped ladder array has the effect of destabilizing synchronization for ranges of values of μ_L, the ratio of the mutual to self-inductance. These specific ranges of μ_L that lead to unstable behavior are geometry dependent. An analytic calculation of the Floquet exponents based on the horizontal junctions agrees with the numerical exponents, based on the full RCSJ equations, for those values of μ_L for which stable phase locking occur. To understand the cause of all the observed instabilities, however, it is crucial in the analytic work to consider the behavior of the vertical junctions.

Although some values of the mutual inductance used in these simulations can not be obtained in simple ladder arrays, this work suggests that experimentalists may wish to attempt fabrication of arrays that enhances the mutual over the self-inductance, perhaps making it possible to look for the rich dynamical behavior predicted here. Certainly researchers working on the problem of coherent emission from Josephson junction arrays should be aware this potential for unstable behavior exists.

The authors wish to thank Barbara Andereck, Tom Dillman, Steve Herbert, Mark Jarrell, and David Stroud for useful conversations. This research was funded by the Howard Hughes Medical Institute Undergraduate Biological Sciences Education Program Grant No. 71196-529503 to Ohio Wesleyan University.

[1] P. Barbara, A. B. Cawthorne, S. V. Shitov, and C. J. Lobb, Phys. Rev. Lett. **82**, 1963 (1999); M. Basler, W. Krech, and K.Y. Platov, Phys. Rev. B **58**, 3409 (1998); K. Wiesenfeld, S. P. Benz, and P. A. A. Booi, J. Appl. Phys. **76**, 3835 (1994).

[2] P. Binder, D. Abraimov, A. V. Ustinov, S. Flach, and Y. Zolotaryuk, Phys. Rev. Lett. **84**, 745 (2000); E. Trías, J. J. Mazo, and T. P. Orlando, *ibid.* **84**, 741 (2000).

[3] S. Ryu, W. Yu, and D. Stroud, Phys. Rev. E **53**, 2190 (1996).

[4] S. F. Mingaleev, Yu. B. Gaididei, E. Majerníková, and S. Shpyrko, Phys. Rev. E **61**, 4454 (2000), and the references therein.

[5] J. J. Mazo and J. C. Ciria, Phys. Rev. B **54**, 16 068 (1996); D. Domínguez and J. V. José, *ibid.* **53**, 11 692 (1996); A. Majhofer, T. Wolf, and W. Dieterich, *ibid.* **44**, 9634 (1991); J. R. Phillips, H. S. J. van der Zant, J. White, and T. P. Orlando, *ibid.* **50**, 9387 (1994).

[6] J. R. Phillips, H. S. J. van der Zant, J. White, and T. P. Orlando, Phys. Rev. B **47**, 5219 (1993).

[7] B. R. Trees and N. Hussain, Phys. Rev. E **61**, 6415 (2000).